organics

MDPI

Article

Theoretical Insight into the Reversal of Chemoselectivity in Diels-Alder Reactions of α,β-Unsaturated Aldehydes and Ketones Catalyzed by Brønsted and Lewis Acids

Lakhdar Benhamed, Sidi Mohamed Mekelleche * and Wafaa Benchouk

Laboratory of Applied Thermodynamics and Molecular Modeling, Department of Chemistry, Faculty of Science, University of Tlemcen, PB 119, Tlemcen 13000, Algeria; lakhdar.benhamed@mail.univ-tlemcen.dz (L.B.); benchouk_wafaa@mail.univ-tlemcen.dz (W.B.)

* Correspondence: sm_mekelleche@mail.univ-tlemcen.dz

Abstract: Experimentally, a reversal of chemoselectivity has been observed in catalyzed Diels–Alder reactions of α,β-unsaturated aldehydes (e.g., (2E)-but-2-enal) and ketones (e.g., 2-hexen-4-one) with cyclopentadiene. Indeed, using the triflimidic Brønsted acid Tf_2NH as catalyst, the reaction gave a Diels–Alder adduct derived from α,β-unsaturated ketone as a major product. On the other hand, the use of tris(pentafluorophenyl)borane $B(C_6F_5)_3$ bulky Lewis acid as catalyst gave mainly the cycloadduct of α,β-unsaturated aldehyde as a major product. Our aim in the present work is to put in evidence the role of the catalyst in the reversal of the chemoselectivity of the catalyzed Diels–Alder reactions of (2E)-but-2-enal and 2-Hexen-4-one with cyclopentadiene. The calculations were performed at the ωB97XD/6-311G(d,p) level of theory and the solvent effects of dichloromethane were taken into account using the PCM solvation model. The obtained results are in good agreement with experimental outcomes.

Keywords: Diels–Alder reaction; chemoselectivity; catalyst; Brønsted acid; Lewis acid; ωB97XD

Citation: Benhamed, L.; Mekelleche, S.M.; Benchouk, W. Theoretical Insight into the Reversal of Chemoselectivity in Diels-Alder Reactions of α,β-Unsaturated Aldehydes and Ketones Catalyzed by Brønsted and Lewis Acids. *Organics* **2021**, *2*, 38–49. https://doi.org/10.3390/org2010004

Academic Editor: Radomir Jasinski

Received: 29 December 2020
Accepted: 2 March 2021
Published: 5 March 2021

1. Introduction

Cycloadditions are one of the strongest bond-forming reactions to prepare (hetero)cyclic molecules in organic synthesis [1–10]. Their usefulness arises from their versatility and remarkable selectivity. Many synthetic routes to cyclic compounds are made possible through Diels–Alder (DA) reactions, which can involve a large variety of dienes and dienophiles [6,11,12]. In addition, various DA reactions have been studied theoretically using computational chemistry tools [13–21]. Notably the molecular electron density theory (MEDT) [22], proposed by Domingo in 2016, has recently become an important tool for the mechanistic study of cycloaddition reactions, about which an important number of papers were published in the last few years [23–32]. According to MEDT, changes in the electron density are responsible for the feasibility of an organic reaction in contrast to the frontier molecular orbital (FMO) theory [33], which uses molecular orbital interactions. Moreover, several quantum-chemical tools are used in MEDT, namely, reactivity indices derived from the conceptual density functional theory (CDFT) [34,35], the topological analysis of the electron localization function (ELF) [36], and the quantum theory of atoms in molecules (QTAIM) [37], to rigorously study organic chemical reactivity on the basis of electron density.

In order to make the cycloaddition feasible, various catalysts are introduced in reactions. Lewis acid (LA) and Brønsted acid (BA) catalysts [38–42] considerably extend the useful scope of DA reactions, enhancing the reaction rate and leading to significant changes in chemo-, regio-, and stereo-selectivities in comparison with the uncatalyzed process [43,44]. A large number of experimental works has been carried out to understand the effects of LA catalysts on the selectivity and the nature of molecular mechanisms of DA

reactions [45–48]. As acidity of the BA can promote highly selectivity in DA cycloadditions, many works on this topic were also published [49–54]. Of note is that the design and development of powerful catalysts is one of the ongoing challenges in modern synthetic chemistry and is very important for the synthesis of natural products, pharmaceuticals, and agrochemicals [55–58].

In 2005, Yamamoto et al. [59] reported a famous work showing high chemoselectivity in the DA cycloaddition of α,β-unsaturated aldehydes 1 and α,β-unsaturated ketones 2 with cyclopentadiene (Cp), where an unexpected reversal of chemoselectivity, according to the choice of the acid catalyst, was observed (Scheme 1).

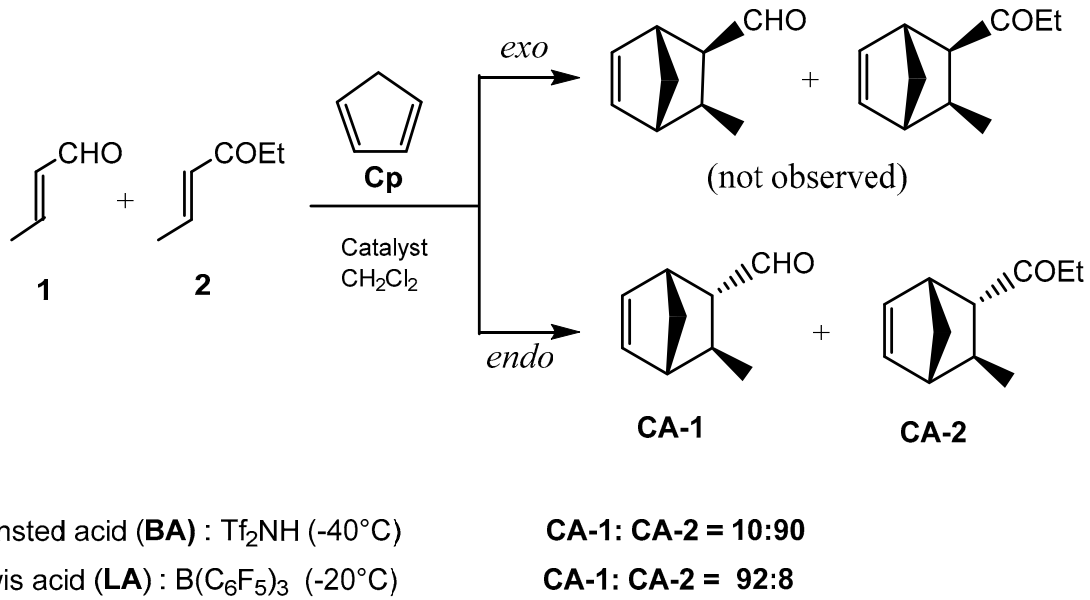

Scheme 1. Chemoselective DA reactions of (2E)-but-2-enal **1** and 2-hexen-4-one **2** with **Cp**. Only the *endo* cycloadducts were experimentally observed.

When a strong BA, such as Tf_2NH, was used as a catalyst, the DA adduct derived from the α,β-unsaturated ketone was obtained as a major product. However, when a bulky LA, such as $B(C_6F_5)_3$, was used as a catalyst, the cycloadduct derived from the α,β-unsaturated aldehyde was the major product. Yamamoto et al. [59] rationalized this reversal of chemoselectivity by the choice of the acid catalyst by consideration of the basicity of the electrophile and the steric hindrance of the acid catalyst. According to the experimentalist, a bulky LA such as $B(C_6F_5)_3$ preferentially coordinates to the sterically less demanding α,β-unsaturated aldehyde, whereas aBA could be regarded as the smallest LA, which would be insensitive to the steric effect. Therefore, a BA selectively coordinates a more basic carbonyl group such as α,β-unsaturated ketone. To the best of our knowledge, the chemoselectivity between LA and BA on this type of DA reaction has not been studied theoretically. Our aim in this contribution is to explore the competitive reactions between the aldehyde **1** and ketone **2** with **Cp** catalyzed by BA and LA catalysts to shed light on the origin of catalytic efficiencies and chemoselectivity details of these reactions using DFT calculations. The competitive chemoselective pathways of this studied reaction are illustrated in Scheme 2.

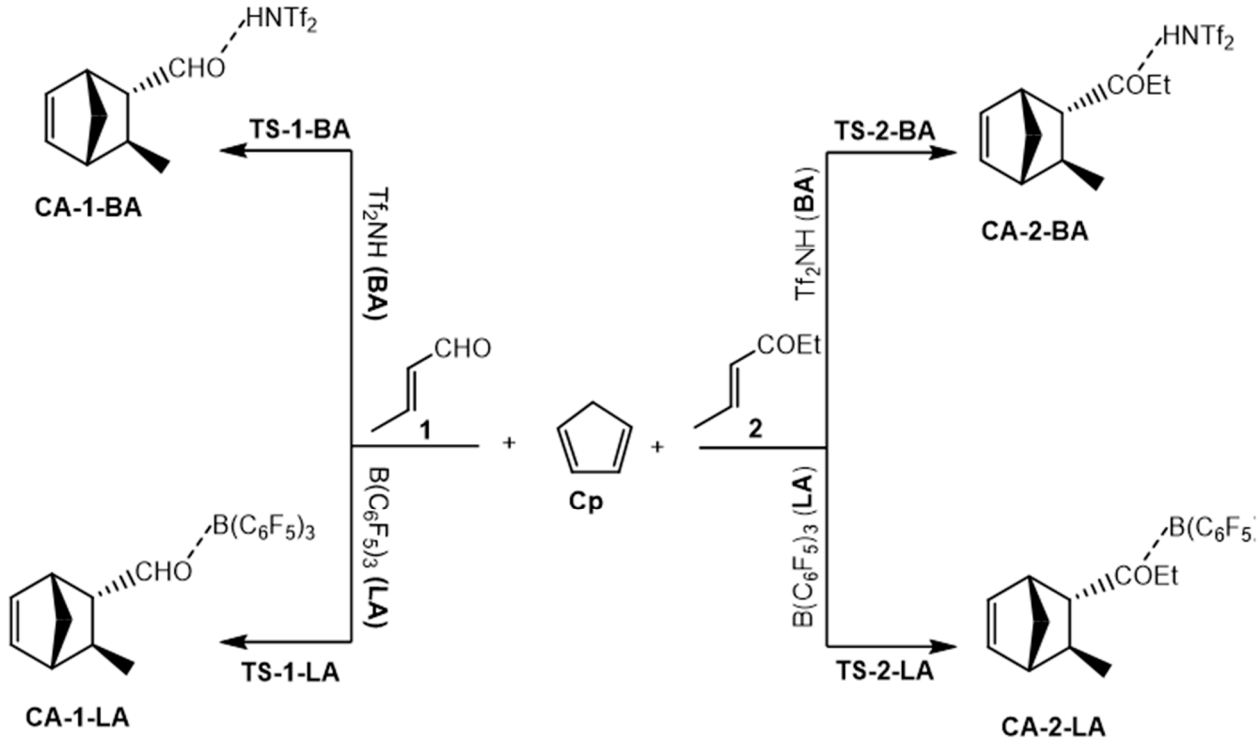

Scheme 2. Competitive chemoselective pathways of the BA-/LA-catalyzed DA reactions of (2E)-but-2-enal **1** and 2-hexen-4-one **2** with **Cp**.

2. Computational Details

All DFT calculations were carried out with the DFT/ωB97XD functional [60] combined with the 6-311G(d,p) basis set [61] implemented in the Gaussian 09 suite of programs [62]. This level of theory has shown to be suitable for geometry optimization and electronic property analysis of (3 + 2) cycloaddition and (4 + 2) DA reactions [17,63,64]. Optimizations were performed using the Berny analytical gradient optimization method [65,66] and the stationary points were characterized by frequency computations in order to verify that the transition states had one and only one imaginary frequency. Solvent effects were analyzed by optimizing the geometries in dichloromethane (DCM) through the polarizable continuum model (PCM) developed in the framework of the self-consistent reaction field (SCRF) [67–70]. The global electron density transfer (GEDT) [71] was computed as a sum of the natural atomic charge, obtained by a natural population analysis (NPA) [72,73] of the atoms belonging to each framework (f) at the TSs, i.e., GEDT (f) = $\sum_{q \in f} q$. Global reactivity indices derived from CDFT [74–81], namely the electrophilicity index ω and the nucleophilicity index N, were calculated using the following expressions [74]:

$$\omega = \frac{\mu 2}{2\eta}$$
$$N \approx \varepsilon_{HOMO}(Nucleophile) - \varepsilon_{HOMO}(TCE)$$
$$\mu \approx (\varepsilon_{HOMO} + \varepsilon_{LUMO})/2$$
$$\eta \approx \varepsilon_{LUMO} - \varepsilon_{HOMO}$$

where TCE = tetracyanoethylene.

3. Results and Discussion

In order to explain the role of the catalyst on the reversal of the chemoselectivity of the catalyzed DA cycloaddition reaction of the α,β–unsaturated aldehyde **1** and α,β–unsaturated ketone **2** with **Cp**, all the chemoselective pathways were investigated (Scheme 2). The studied DA reactions were:

(i) **1** + **Cp** in the absence and presence of the BA/LA catalysts; and
(ii) **2** + **Cp** in the absence and presence of the BA/LA catalysts.

The quantum chemical calculations are based on the analysis of CDFT reactivity indices and calculated activation energies and free energies. The polarity of the cycloaddition processes is quantified by GEDT calculations at the located TSs.

3.1. Analysis of the Global CDFT-Based Reactivity Indexes

Global indexes defined in the context of the CDFT [34,35], namely, the electronic chemical potential μ, chemical hardness η, global electrophilicity ω, and nucleophilicity N, were calculated in terms of the one electron energies of the HOMO/LUMO frontier molecular orbitals at the ground states of the reactants in gas phase. The following table recapitulates the global reactivity indices for uncatalyzed reactants **1** and **2**, BA-catalyzed reactants **1-BA** and **2-BA**, and LA-catalyzed reactants **1-LA** and **2-LA** (Table 1).

Table 1. ωB97XD/6-311G(d,p) global electronic properties (chemical potential μ, chemical hardness η, electrophilicity ω, nucleophilicity N) of uncatalyzed reactants **1** and **2**, BA-catalyzed reactants **1-BA** and **2-BA**, and LA-catalyzed reactants **1-LA** and **2-LA**, in gas phase.

	Global Properties (in eV)				
	μ	η	ω	N	$\Delta\omega$ [1]
Cp	−0.123	0.352	0.58	3.63	0.00
1	−0.162	0.351	1.02	2.56	0.44
2	−0.156	0.350	0.94	2.76	0.36
1-BA	−0.201	0.362	1.52	1.36	0.94
2-BA	−0.193	0.367	1.40	1.60	0.82
1-LA	−0.197	0.256	2.05	2.91	1.47
2-LA	−0.192	0.265	1.89	2.94	1.31

[1] Relative to **Cp**.

It turned out that the electronic chemical potential μ [34,82] of **Cp**, −0.123 eV, was higher than that of the uncatalyzed and catalyzed aldehyde and ketone, indicating that along the cycloaddition reaction the electron density will flux from the diene **Cp** to the dienophile aldehyde/ketone, being classified as the forward electron density flux (FEDF) [83]. The electrophilicity ω index [35] of **Cp**, 0.58 eV, being classified as a weak electrophile, was lower than that of uncatalyzed and catalyzed aldehyde and ketone. In the absence of catalysts, aldehyde **1** (ω = 1.02 eV) and ketone **2** (ω = 0.94 eV) can be classified as moderate electrophiles [74]. By introducing the BA catalyst, the electrophilicity of the dienophiles increased. It became 1.52 eV for BA-catalyzed aldehyde **1-BA** and 1.40 eV for BA-catalyzed ketone **2-BA.** By substituting the BA catalyst by the LA catalyst, the electrophilicities increased and reached 2.05 eV for LA-catalyzed aldehyde **1-LA** and 1.89 eV for LA-catalyzed ketone **2-LA**, which made them strong electrophiles although the aldehyde was predicted to be more electrophile than the ketone in the absence and presence of BA/LA catalysts.

The nucleophilicity N index [84,85] of **Cp**, 3.63 eV, was higher than that of the uncatalyzed aldehyde **1** (N = 2.56 eV) and ketone **2** (N = 2.76 eV), indicating that **Cp** acted as a nucleophile and dienophiles **1** and **2** acted as electrophiles. In the presence of **BA**, the nucleophilicity of the catalyzed aldehyde **1-BA** and ketone **2-BA** was reduced to 1.36 and 1.60 eV, respectively. Contrariwise, in the presence of LA, the nucleophilicity of the catalyzed aldehyde **1-BA** and ketone **2-BA** was increased to 2.91 and 2.94 eV, respectively. The difference in electrophilicity, $\Delta\omega$, for the DA reactions (**1** + **Cp**), (**1-BA** + **Cp**), and (**1-LA** + **Cp**) were 0.44 eV, 0.94 eV, and 1.47 eV, respectively, indicating the largest polarity of the cycloaddition reaction between the aldehyde **1** and **Cp** corresponded to the **1-LA** + **Cp** catalyzed reaction. The same trends were found for the DA reactions between the ketone **2** and **Cp**. In conclusion, compared to the uncatalyzed and BA-catalyzed DA reactions, the LA-catalyzed DA reactions were predicted to be the most polar ones.

*3.2. Analysis of the Potential Energy Surface of the Uncatalyzed and Catalyzed DA Reactions of **1** and **2***

3.2.1. Competitive Uncatalyzed DA Reactions of **1** and **2** with Cp

The competitive DA reactions between α,β-unsaturated aldehyde **1** with **Cp** and between α,β-unsaturated ketone **2** with **Cp** (Scheme 1) were studied first in the absence of catalysts. The first DA reaction of **1** with **Cp** led to the formation of the cycloadduct **CA-1** via **TS-1** and the second DA reaction of **2** with **Cp** led to the formation of the cycloadduct **CA-2** via **TS-2**. The gas phase energies and Gibbs free energies in DCM at −40 °C (experimental conditions of BA-catalyzed reaction) and at −20 °C (experimental conditions of LA-catalyzed reaction) are summarized in Table 2 and the chemical structures of the gas phase TSs, drawn using GaussView 5.0 [86], are given in Figure 1a.

Table 2. Total energies E and relative energies ΔE in gas phase, and free energies G° and relative free energies ΔG° in solvent for the uncatalyzed DA reactions (**1** + **Cp**) and (**2** + **Cp**).

	Gas Phase		In DCM at −40 °C		DCM at −20 °C	
	E (in a.u.)	**ΔE (in kcal/mol)**	**G° (in a.u.)**	**ΔG° (in kcal/mol)**	**G° (in a.u.)**	**ΔG° (in kcal/mol)**
Cp	−194.081227		−194.010442		−194.012466	
1	−231.214513		−231.151897		−231.154155	
2	−309.848932		−309.732115		−309.734767	
1 + Cp	−425.295740	0.0	−425.162339	0.0	−425.166621	0.0
2 + Cp	−503.930160	0.0	−503.742557	0.0	−503.747233	0.0
TS-1	−425.268971	16.8 [1]	−425.115299	29.5 [1]	−425.118053	30.5 [1]
TS-2	−503.904754	**15.9** [2]	−503.695977	**29.2** [2]	−503.699094	**30.2** [2]
CA-1	−425.337504	−26.2 [1]	−425.178925	−10.4 [1]	−425.176228	−6.0 [1]
CA-2	−503.975693	−28.6 [2]	−503.762314	−12.4 [2]	−503.759272	−7.5 [2]

[1] Relative to reactants (**1** + **Cp**); [2] relative to reactants (**2** + **Cp**).

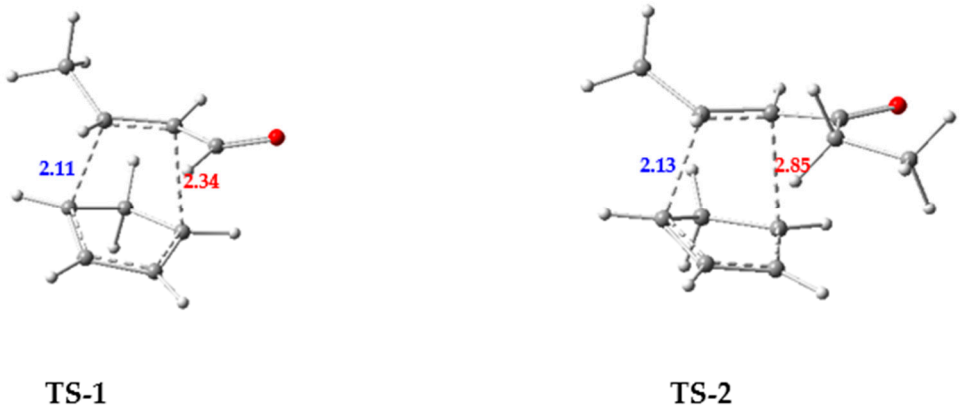

(**a**) Uncatalyzed reactions in gas phase.

Figure 1. *Cont.*

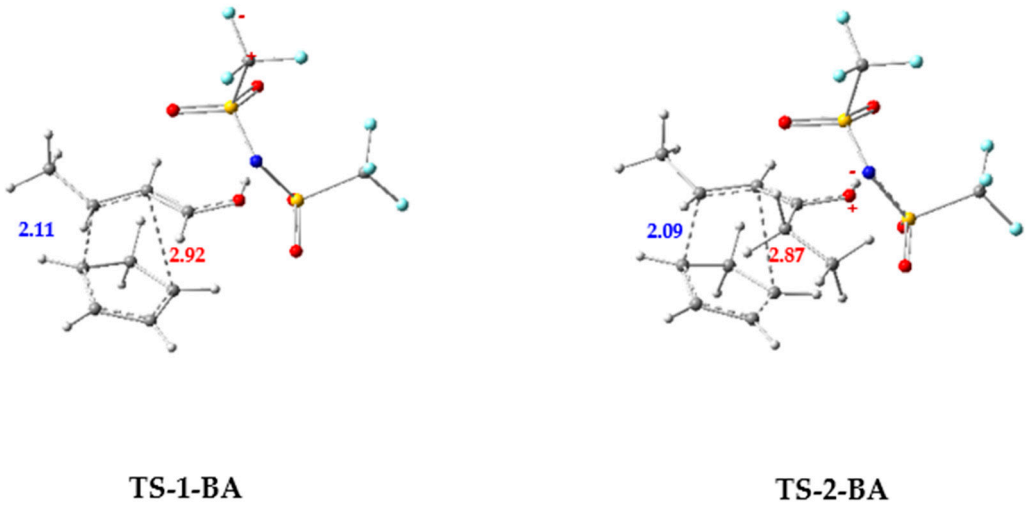

(**b**) BA-catalyzed reactions in DCM at −40 °C.

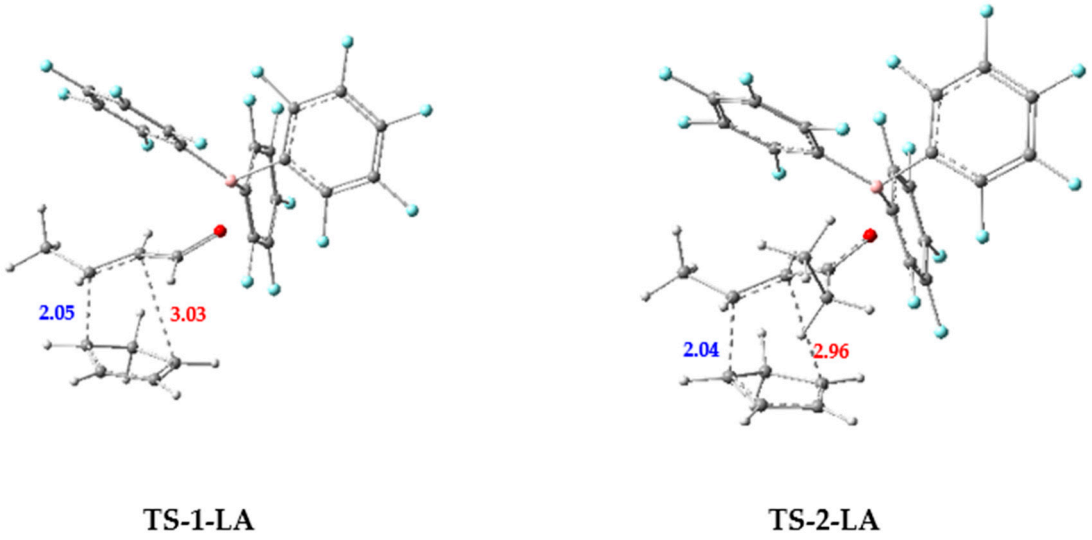

(**c**) LA-catalyzed reactions in DCM at −20 °C.

Figure 1. ωB97XD/6-311G(d,p) geometries of transition state structures involved in chemoselective DA reactions: (**a**) uncatalyzed reactions (**1** + **Cp**) and (**2** + **Cp**), (**b**) BA-catalyzed reactions (**1-BA** + **Cp**) and (**2-BA** + **Cp**), and (**c**) LA-catalyzed reactions (**1-LA** + **Cp**) and (**2-LA** + **Cp**). The bond lengths are given in Angstroms.

The calculated activation barriers in gas phase and in DCM show that the second DA reaction (**2** + **Cp**) was kinetically more favored than the first DA reaction (**1** + **Cp**) by 0.9, 0.3, and 0.3 kcal/mol in gas phase, DCM at −40 °C, and DCM at −20 °C, respectively. We also noted that the second DA reaction was found to be more exergonic than the first one by 2.0 and 1.5 kcal/mol in DCM at −40 °C and −20 °C, respectively.

3.2.2. BA-Catalyzed DA Reactions of 1-BA and 2-BA with Cp

In the presence of the triflimide Tf_2NH as a BA catalyst, the competitive DA reactions of BA-catalyzed aldehyde **1-BA** and BA-catalyzed ketone **2-BA** with **Cp**, giving **CA-1-BA** via **TS-1-BA** and **CA-2-BA** via **TS-2-BA** respectively, were studied. Calculations were

carried out in gas phase and in DCM at −40 °C. The results are summarized in Table 3 and the chemical structures of TSs in solvent are given in Figure 1b.

Table 3. Total energies E and relative energies ΔE in gas phase, and free energies G° and relative free energies ΔG° in solvent for the possible chemo pathways of DA reactions catalyzed by BA. The enthalpy and entropy contributions of ΔG° are included.

	Gas Phase		In DCM at −40 °C			
	E (in a.u.)	**ΔE (in kcal/mol)**	**G° (in a.u.)**	**ΔG° (in kcal/mol)**	**ΔH° (in kcal/mol)**	**−TΔS° (in kcal/mol)**
Cp	−194.081227		−194.010442			
1-BA	−2058.968156		−2058.860635			
2-BA	−2137.604500		−2137.442545			
1-BA + Cp	−2253.049384	0.0	−2252.871077	0.0		
2-BA + Cp	−2331.685728	0.0	−2331.452987	0.0		
TS-1-BA	−2253.033186	10.2 [1]	−2252.847153	15.0 [1]	2.6 (17.5%)	12.4 (82.5%)
TS-2-BA	−2331.670205	**9.7** [2]	−2331.430226	**14.3** [2]	2.1 (14.9%)	12.2 (85.1%)
CA-1-BA	−2253.094037	−28.0 [1]	−2252.885020	−8.7 [1]		
CA-2-BA	−2331.733508	−30.0 [2]	−2331.471355	−11.5 [2]		

[1] Relative to reactants (**1-BA** + **Cp**); [2] relative to reactants (**2-BA** + **Cp**).

Introducing Tf_2NH as BA catalyst, the calculated activation barriers in gas phase and in DCM at −40 °C show that the second DA reaction (**2-BA** + **Cp**) was kinetically more favored than the first DA reaction (**1-BA** + **Cp**) by 0.5 and 0.7 kcal/mol in gas phase and DCM at −40 °C, respectively. We also noted that the second DA reaction was found to be more exergonic than the first one by 2.8 kcal/mol in DCM at −40 °C, which is in good agreement with experimental outcomes.

3.2.3. LA-Catalyzed Reaction of 1-LA and 2-LA with Cp

In the presence of the LA tris(pentafluorophenyl)borane $B(C_6F_5)_3$, catalyzed DA reactions of aldehyde **1-LA** and ketone **2-LA** with **Cp**, giving cycloadduct **CA-1-LA** and **CA-2-LA** via **TS-1-LA** and **TS-2-LA**, respectively, were studied. Calculations were carried out in gas phase and in DCM at −20 °C. The results are summarized in Table 4 and the chemical structures of TSs in solvent are given in Figure 1c.

Table 4. Total energies E and relative energies ΔE in gas phase, and free energies G° and relative free energies ΔG° in solvent for the possible chemo pathways of DA reactions catalyzed by LA. The enthalpy and entropy contributions of ΔG° are included.

	Gas Phase		In DCM at −20 °C			
	E (in a.u.)	**ΔE (in kcal/mol)**	**G° (in a.u.)**	**ΔG° (in kcal/mol)**	**ΔH° (in kcal/mol)**	**−TΔS° (in kcal/mol)**
Cp	−194.081227		−194.010442			
1-LA	−2439.454482		−2439.272585			
2-LA	−2518.095162		−2517.856115			
1-LA + Cp	−2633.535709	0.0	−2633.283027	0.0		
2-LA + Cp	−2712.176389	0.0	−2711.866557	0.0		
TS-1-LA	−2633.525405	6.5 [1]	−2633.258044	**15.7** [1]	5.2 (33.3%)	10.5 (66.7%)
TS-2-LA	−2712.169099	**4.6** [2]	−2711.840294	16.5 [2]	5.0 (30.4%)	11.5 (69.6%)
CA-1-LA	−2633.576707	−25.7 [1]	−2633.295055	−7.5 [1]		
CA-2- LA	−2712.223191	−29.4 [2]	−2711.882229	−9.8 [2]		

[1] Relative to reactants (**1-LA** + **Cp**); [2] relative to reactants (**2-LA** + **Cp**).

In opposition to the Tf_2NH-catalyzed DA reactions, the $B(C_6F_5)_3$-catalyzed DA reactions led to a reversed chemoselectivity. Indeed, in DCM at −20 °C, the calculated activation barriers indicate that the activation free energy for the DA reaction **1-LA** + **Cp**,

15.7 kcal/mol, was lower than that of the DA reaction **2-LA** + **Cp**, 16.5 kcal/mol, indicating that chemo pathway involving the catalyzed aldehyde was kinetically more favored than the chemo pathway involving the catalyzed ketone, in agreement with experiment. We noted that the calculations performed in gas phase did not reproduce the experimental finding, showing the importance of solvent effects in the calculation of activation barriers. We also noted that the two competitive chemo pathways were exergonic. It is important to note that intrinsic reaction coordinate (IRC) calculations indicated that the studied DA reactions followed a one-step mechanism and the eventuality of a stepwise mechanism was excluded. Indeed, the optimization of the last structures on the IRC curves in the forward direction gave structures identical to those of cycloadducts, indicating the absence of stable reaction intermediates.

To quantify the electronic and steric effects of BA and LA catalysts on the chemoselectivity of the studied DA reactions, we calculated the enthalpic and entropic contributions by partitioning **ΔG°** into two terms: ΔH° and −TΔS° (Tables 3 and 4). According to the obtained results, we concluded that (i) both the steric and electronic effect are important in BA- and LA-catalyzed DA reactions; (ii) the steric contribution is more important than the electronic contribution in both BA- and LA-catalyzed reactions; (iii) the electronic contributions for LA-catalyzed reactions, 33.3% and 30.4%, are more important than those of BA-catalyzed reactions (17.5% and 14.9%); (iv) for BA-catalyzed reactions, the steric contribution in **TS-2-BA** is more important than in **TS-1-BA;** and (v) in LA-catalyzed reactions, there is a decrease of steric contribution and increase of electronic contribution compared to BA-catalyzed reactions.

3.3. Relative Activation Free Energies and Boltzmann–Maxwell Populations

Table 5 summarizes the relative activation of Gibbs free energies, **ΔΔG°,** for the TSs corresponding to the four competitive chemo pathways, namely, **1-BA + Cp, 2-BA + Cp**, **1-LA + Cp,** and **2-LA + Cp** reported in Tables 3 and 4. The Maxwell–Boltzmann populations defined by $[B]/[A] = \exp(-\Delta\Delta G/RT)$ for the two equilibriums **TS-1-BA** ⇌ **TS-2-BA** and **TS-1-LA** ⇌ **TS-2-LA** were also calculated and are recapitulated in Table 5.

Table 5. Relative free energies ΔΔG° (in kcal/mol) between barrier free energies ΔG° of TSs in DCM and their corresponding Boltzmann–Maxwell populations (%).

	In DCM at −40 °C		**in DCM at −20 °C**	
	ΔΔG° pop(%)		**ΔΔG° pop(%)**	
TS-1-BA	0.7	17.14		
TS-2-BA	0.0	82.86		
TS-1-LA			0.0	83.07
TS-2-LA			0.8	16.93

In the case of the BA-catalyzed reactions, the calculated Maxwell–Boltzmann populations shows that the population of **TS-2-BA** represented 82.86% of the mixture, whereas the population of **TS-1-BA** represented only 17.14%, indicating that chemo pathway **2-BA** + **Cp** was kinetically more favored than the chemo pathway **1-BA** + **Cp** in DCM at −40 °C. By contrast, in the case of the LA-catalyzed reactions, the calculated Maxwell–Boltzmann populations show that the population of **TS-1-LA** represented 83.07% of the mixture, whereas the population of **TS-2-LA** represented only 16.93%, indicating chemo pathway **1-LA** + **Cp** was kinetically more favored than chemo pathway **2-LA** + **Cp** in DCM at −20 °C. The obtained results put in evidence the crucial role played by the type of catalyst in the reversal of chemoselectivity in catalyzed DA reactions of α,β-unsaturated aldehydes.

3.4. GEDT Analysis and Polarity

The global electron density transfers (GEDTs) [71] were estimated from natural population analysis (NPA) [72,73] at the located TSs. The calculated GEDTs for uncatalyzed and BA/LA-catalyzed DA reactions are summarized in Table 6.

Table 6. GEDT (given in e) of the uncatalyzed and BA-/LA-catalyzed DA reactions.

	Uncatalyzed DA Reactions		**BA-Catalyzed DA Reactions**		**LA-Catalyzed DA Reactions**	
	TS-1	**TS-2**	**TS-1-BA**	**TS-2-BA**	**TS-1-LA**	**TS-2-LA**
GEDT	0.13	0.12	0.26	0.23	0.38	0.33

In the absence of catalysts, the GEDT values at **TS-1** (0.13e) and **TS-2** (0.12e) showed electron density fluxes from **Cp** to aldehyde **1** and ketone **2**. The flux was two times greater in the presence of the BA catalyst and three times greater in the presence of the LA catalyst. These results clearly reveal that both the uncatalyzed and catalyzed studied DA reactions can be classified as polar processes. We noted that the calculated GEDTs (Table 6) correlated well with the calculated activation barriers (Tables 2–4). Indeed, when passing from the uncatalyzed reactions to BA- and LA-catalyzed reactions, an increase in the polarity led to a decrease in activation energies and free energies. We also noted that the calculated GEDTs (Table 6) also correlated well with the calculated electrophilicity differences $\Delta\omega$ (Table 1). Indeed, when passing from the uncatalyzed reactions to BA- and LA-catalyzed reactions, the increase of $\Delta\omega$ values led to an increase in polarity and consequently a decrease in activation barriers.

4. Conclusions

The chemoselectivity of the (un)catalyzed DA reactions of α,β-unsaturated aldehyde **1** and ketone **2** with **Cp** was investigated at the ωB97XD/6-311G(d,p) level of theory. The obtained results show that the most favored chemo pathway depends strongly on the type of the catalyst (Brønsted acid vs. bulky Lewis acid).

(i) In the case of the uncatalyzed DA reactions, the **2** + **Cp** reaction was found to be kinetically more favored than the **1** + **Cp** reaction both in gas phase and in DCM.

(ii) In the case of the DA reactions catalyzed by BA, the **2-BA** + **Cp** reaction was found to be kinetically more favored than the **1-BA** + **Cp** reaction both in gas phase and in DCM at −40 °C. Moreover, the calculated activation barriers, GEDTs at TSs, and electrophilicity differences ($\Delta\omega$) indicated that the BA-catalyzed reactions were predicted to be more polar and faster compared to the uncatalyzed reactions.

(iii) In the case of the DA reactions catalyzed by LA, the **1-LA** + **Cp** reaction was found to be kinetically more favored than the **2-LA** + **Cp** reaction in DCM at −20 °C. In addition, the LA-catalyzed reactions were predicted to be more polar and faster compared to the uncatalyzed and BA-catalyzed reactions.

(iv) The relative free energies and Maxwell–Boltzmann populations of the competitive TSs, calculated in DCM, put in evidence the reversal of the chemoselectivity when the BA catalyst Tf_2NH -was replaced by the bulky LA catalyst $B(C_6F_5)_3$, in agreement with the experimental findings.

Author Contributions: Conceptualization: S.M.M.; Investigation: L.B.; S.M.M. and W.B.; Methodology: L.B.; S.M.M.; Supervision: S.M.M.; Writing original draft: L.B. and S.M.M.; Writing—review & editing, L.B. and S.M.M.; All authors have read and agreed to the published version of the manuscript.

Funding: This research was funded by the Ministry of Higher Education and Scientific Research of the Algerian government for the project PRFU B00L01UN130120180001.

Institutional Review Board Statement: Not applicable.

Informed Consent Statement: Not applicable.

Data Availability Statement: Not applicable.

Conflicts of Interest: The authors declare no conflict of interest.

References

1. Huisgen, R. Cycloadditions—Definition, Classification, and Characterization. *Angew. Chem. Int. Ed.* **1968**, *7*, 321–328. [CrossRef]
2. Padwa, A. *1,3-Dipolar Cycloaddition Chemistry*; Padwa, A., Ed.; John Wiley and Sons: New York, NY, USA, 1984.
3. Frühauf, H.-W. Metal-Assisted Cycloaddition Reactions in Organotransition Metal Chemistry. *Chem. Rev.* **1997**, *97*, 523–596. [CrossRef] [PubMed]
4. Kobayashi, S.; Jørgensen, K.A. Frontmatter and Index. In *Cycloaddition Reactions in Organic Synthesis*; Kobayashi, S., Jørgensen, K.A., Eds.; Wiley-VCH Verlag GmbH: Weinheim, Germany, 2001. [CrossRef]
5. Nicolaou, K.C.; Snyder, S.A.; Montagnon, T.; Vassilikogiannakis, G. The Diels-Alder Reaction in Total Synthesis. *Angew. Chem. Int. Ed.* **2002**, *41*, 1668–1698. [CrossRef]
6. Fringuelli, F.; Taticchi, A. *The Diels-Alder Reaction: Selected Practical Methods*; Fringuelli, F., Taticchi, A., Eds.; Wiley: Chichester, UK; New York, NY, USA, 2002.
7. Konovalov, A.I.; Kiselev, V.D. Diels-Alder Reaction. Effect of Internal and External Factors on the Reactivity of Diene—Dienophile Systems. *Russ. Chem. Bull.* **2003**, *52*, 293–311. [CrossRef]
8. Hodgson, D.M.; Labande, A.H.; Muthusamy, S. Cycloadditions of Carbonyl Ylides Derived from Diazocarbonyl Compounds. In *Organic Reactions*; Denmark, S.E., Ed.; John Wiley & Sons, Inc.: Hoboken, NJ, USA, 2012; Chapter 2, pp. 133–496. [CrossRef]
9. Ylijoki, K.E.O.; Stryker, J.M. [5+2] Cycloaddition Reactions in Organic and Natural Product Synthesis. *Chem. Rev.* **2013**, *113*, 2244–2266. [CrossRef]
10. Martel, A.; Dhall, R.; Gaulon, C.; Laurent, M.Y.; Dujardin, G. Dihydrofurans by cycloadditions of oxadienes. In *Organic Reactions*, 1st ed.; Weinreb, S.M., Ed.; John Wiley & Sons, Inc.: Hoboken, NJ, USA, 2004; Chapter 1; pp. 1–916. [CrossRef]
11. Boger, D.L. Diels-Alder reactions of heterocyclic aza dienes. Scope and applications. *Chem. Rev.* **1986**, *86*, 781–793. [CrossRef]
12. Hayashi, Y. Catalytic Asymmetric Diels-Alder Reactions. In *Cycloaddition Reactions in Organic Synthesis*; Kobayashi, S., Jørgensen, K.A., Eds.; Wiley-VCH Verlag GmbH: Weinheim, Germany, 2001; Chapter 1; pp. 5–55. [CrossRef]
13. Houk, K.N.; Loncharich, R.J.; Blake, J.F.; Jorgensen, W.L. Substituent effects and transition structures for Diels-Alder reactions of butadiene and cyclopentadiene with cyanoalkenes. *J. Am. Chem. Soc.* **1989**, *111*, 9172–9176. [CrossRef]
14. Jorgensen, W.L.; Lim, D.; Blake, J.F. Ab initio study of Diels-Alder reactions of cyclopentadiene with ethylene, isoprene, cyclopentadiene, acrylonitrile, and methyl vinyl ketone. *J. Am. Chem. Soc.* **1993**, *115*, 2936–2942. [CrossRef]
15. Domingo, L.R.; Sáez, J.A. Understanding the mechanism of polar Diels-Alder reactions. *Org. Biomol. Chem.* **2009**, *7*, 3576–3585. [CrossRef] [PubMed]
16. Morales-Bayuelo, A.; Vivas-Reyes, R. Understanding the Polar Character Trend in a Series of Diels-Alder Reactions Using Molecular Quantum Similarity and Chemical Reactivity Descriptors. *J. Quantum Chem.* **2014**, *2014*. [CrossRef]
17. Cui, C.-X.; Liu, Y.-J. A thorough understanding of the Diels-Alder reaction of 1,3-butadiene and ethylene: Diels-Alder reaction of 1,3-butadiene and ethylene. *J. Phys. Org. Chem.* **2014**, *27*, 652–660. [CrossRef]
18. Levandowski, B.J.; Houk, K.N. Theoretical Analysis of Reactivity Patterns in Diels-Alder Reactions of Cyclopentadiene, Cyclohexadiene, and Cycloheptadiene with Symmetrical and Unsymmetrical Dienophiles. *J. Org. Chem.* **2015**, *80*, 3530–3537. [CrossRef]
19. Jasiński, R. A reexamination of the molecular mechanism of the Diels-Alder reaction between tetrafluoroethene and cyclopentadiene. *React. Kinet. Mech. Catal.* **2016**, *119*, 49–57. [CrossRef]
20. Chen, S.; Yu, P.; Houk, K.N. Ambimodal Dipolar/Diels-Alder Cycloaddition Transition States Involving Proton Transfers. *J. Am. Chem. Soc.* **2018**, *140*, 18124–18131. [CrossRef]
21. Jasiński, R.; Kwiatkowska, M.; Barański, A. Stereoselectivity and kinetics of [4+2] cycloaddition reaction of cyclopentadiene to para-substituted E-2-arylnitroethenes. *J. Phys. Org. Chem.* **2011**, *24*, 843–853. [CrossRef]
22. Domingo, L. Molecular Electron Density Theory: A Modern View of Reactivity in Organic Chemistry. *Molecules* **2016**, *21*, 1319. [CrossRef] [PubMed]
23. Domingo, L.R.; Ríos-Gutiérrez, M.; Pérez, P. A Molecular Electron Density Theory Study of the Competitiveness of Polar Diels-Alder and Polar Alder-ene Reactions. *Molecules* **2018**, *23*, 1913. [CrossRef] [PubMed]
24. Domingo, L.R.; Acharjee, N. Molecular Electron Density Theory: A New Theoretical Outlook on Organic Chemistry. In *Frontiers in Computational Chemistry*; Ul-Haq, Z., Wilson, A.K., Eds.; Bentham Science Publishers: Sharjah, UAE, 2020; Chapter 2; pp. 174–227. [CrossRef]
25. Acharjee, N.; Banerji, A. A molecular electron density theory study to understand the interplay of theory and experiment in nitrone-enone cycloaddition. *J. Chem. Sci.* **2020**, *132*, 65. [CrossRef]
26. Benhamed, L.; Mekelleche, S.M.; Benchouk, W.; Charif, I.E.; Ríos-Gutiérrez, M.; Domingo, L.R. Understanding the Influence of the Trifluoromethyl Group on the Selectivities of the [3+2] Cycloadditions of Thiocarbonyl S -methanides with α, β-Unsaturated Ketones. A MEDT study. *ChemistrySelect* **2020**, *5*, 12791–12806. [CrossRef]
27. Domingo, L.R.; Ríos-Gutiérrez, M. On the nature of organic electron density transfer complexes within molecular electron density theory. *Org. Biomol. Chem.* **2019**, *17*, 6478–6488. [CrossRef]

28. Emamian, S.; Domingo, L.R.; Javad Hosseini, S.; Ali-Asgari, S. A Study of the Effects of the Lewis Acid Catalysts on Oxa-Diels-Alder Reactions through Molecular Electron Density Theory. *ChemistrySelect* **2020**, *5*, 5341–5348. [CrossRef]
29. Hosseini, S.J. Exploring effects of the trifluoromethyl substituent on the chemoselectivity and regioselectivity of [3+2] cycloadditions of thiocarbonyl S-methanides with α, β-unsaturated ketones. *J. Chin. Chem. Soc.* **2020**, *67*, 703–710. [CrossRef]
30. Jalali, H.; Hosseini, S.J.; Ali-Asgari, S.; Izadi Nia, J. Stereoselective aziridination of imines via ammonium ylides: A molecular electron density theory study. *J. Heterocycl. Chem.* **2020**, *57*, 419–427. [CrossRef]
31. Ríos-Gutiérrez, M.; Nasri, L.; Khorief Nacereddine, A.; Djerourou, A.; Domingo, L.R. A molecular electron density theory study of the [3+2] cycloaddition reaction between an azomethine imine and electron deficient ethylenes. *J. Phys. Org. Chem.* **2018**, *31*, e3830. [CrossRef]
32. Barama, L.; Bayoud, B.; Chafaa, F.; Nacereddine, A.K.; Djerourou, A. A mechanistic MEDT study of the competitive catalysed [4+2] and [2+2] cycloaddition reactions between 1-methyl-1-phenylallene and methyl acrylate: The role of Lewis acid on the mechanism and selectivity. *Struct. Chem.* **2018**, *29*, 1709–1721. [CrossRef]
33. Fukui, K. Molecular Orbitals in Chemistry, Physics, and Biology. In *Index to Reviews, Symposia Volumes and Monographs in Organic Chemistry*; Lowdin, P.O., Ed.; Academic Press: New York, NY, USA; London, UK, 1966. [CrossRef]
34. Parr, R.G.; Pearson, R.G. Absolute hardness: Companion parameter to absolute electronegativity. *J. Am. Chem. Soc.* **1983**, *105*, 7512–7516. [CrossRef]
35. Parr, R.G.; Szentpály, L.V.; Liu, S. Electrophilicity Index. *J. Am. Chem. Soc.* **1999**, *121*, 1922–1924. [CrossRef]
36. Becke, A.D.; Edgecombe, K.E. A simple measure of electron localization in atomic and molecular systems. *J. Chem. Phys.* **1990**, *92*, 5397–5403. [CrossRef]
37. Bader, R.F.W. *Atoms in Molecules: A Quantum Theory*; Clarendon Press: Oxford, UK; New York, NY, USA, 1990. [CrossRef]
38. Carruthers, W.; Coldham, I. *Modern Methods of Organic Synthesis*; Carruthers, W., Coldham, I., Eds.; Cambridge University Press: Cambridge, UK, 2004; pp. 159–264.
39. Yamamoto, H.; Boxer, M.B. Super Brønsted Acid Catalysis in Organic Synthesis. *CHIMIA Int. J. Chem.* **2007**, *61*, 279–281. [CrossRef]
40. Cheon, C.H.; Yamamoto, H. Super Brønsted acid catalysis. *Chem. Commun.* **2011**, *47*, 3043. [CrossRef] [PubMed]
41. Yamamoto, H. Acid Catalysis in Organic Synthesis. In *Inventing Reactions*; Gooßen, L.J., Ed.; Springer: Berlin/Heidelberg, Germany, 2012; pp. 315–334. [CrossRef]
42. Ishihara, K. Chiral B (III) Lewis Acids. In *Lewis Acids in Organic Synthesis*; Yamamoto, H., Ed.; Wiley-VCH Verlag GmbH: Weinheim, Germany, 2000; pp. 135–190. [CrossRef]
43. Fringuelli, F.; Piermatti, O.; Pizzo, F.; Vaccaro, L. Recent Advances in Lewis Acid Catalyzed Diels-Alder Reactions in Aqueous Media. *Eur. J. Org. Chem.* **2001**, *17*, 439–455. [CrossRef]
44. Kagan, H.B.; Riant, O. Catalytic asymmetric Diels-Alder reactions. *Chem. Rev.* **1992**, *92*, 1007–1019. [CrossRef]
45. Li, P.; Yamamoto, H. Lewis Acid Catalyzed Inverse-Electron-Demand Diels-Alder Reaction of Tropones. *J. Am. Chem. Soc.* **2009**, *131*, 16628–16629. [CrossRef]
46. Shen, J.; Tan, C.-H. Brønsted-acid and Brønsted-base catalyzed Diels-Alder reactions. *Org. Biomol. Chem.* **2008**, *6*, 3229. [CrossRef]
47. Pindur, U.; Lutz, G.; Otto, C. Acceleration and Selectivity Enhancement of Dlels-Alder Reactions by Special and Catalytic Methods. *Chem. Rev.* **1993**, *93*, 741–761. [CrossRef]
48. Futatsugi, K.; Yamamoto, H. Oxazaborolidine-Derived Lewis Acid Assisted Lewis Acid as a Moisture-Tolerant Catalyst for Enantioselective Diels-Alder Reactions. *Angew. Chem. Int. Ed.* **2005**, *44*, 1484–1487. [CrossRef]
49. Yamamoto, H. From designer Lewis acid to designer Brnsted acid towards more reactive and selective acid catalysis. *Proc. Jpn. Acad. Ser. B* **2008**, *84*, 134–146. [CrossRef]
50. Jung, M.E.; Guzaev, M. Trimethylaluminum-Triflimide Complexes for the Catalysis of Highly Hindered Diels-Alder Reactions. *Org. Lett.* **2012**, *14*, 5169–5171. [CrossRef]
51. Liu, L.; Kim, H.; Xie, Y.; Farès, C.; Kaib, P.S.J.; Goddard, R.; List, B. Catalytic Asymmetric [4+2]-Cycloaddition of Dienes with Aldehydes. *J. Am. Chem. Soc.* **2017**, *139*, 13656–13659. [CrossRef]
52. Zhao, W.; Sun, J. Triflimide ($HNTf_2$) in Organic Synthesis. *Chem. Rev.* **2018**, *118*, 10349–10392. [CrossRef] [PubMed]
53. Held, F.; Grau, D.; Tsogoeva, S. Enantioselective Cycloaddition Reactions Catalyzed by BINOL-Derived Phosphoric Acids and *N*-Triflyl Phosphoramides: Recent Advances. *Molecules* **2015**, *20*, 16103–16126. [CrossRef]
54. Dodziuk, H. *Strained Hydrocarbons: Beyond the van-t Hoff and Le Bel Hypothesis*, 1st ed.; Dodziuk, H., Ed.; Wiley-VCH Verlag Gmbh & Co. KGaA: Weinheim, Germany, 2009. [CrossRef]
55. Park, S.; Sugiyama, H. DNA-Based Hybrid Catalysts for Asymmetric Organic Synthesis. *Angew. Chem. Int. Ed.* **2010**, *49*, 3870–3878. [CrossRef]
56. Megens, R.P.; Roelfes, G. Asymmetric Catalysis with Helical Polymers. *Chem. A Eur. J.* **2011**, *17*, 8514–8523. [CrossRef]
57. Rioz-Martínez, A.; Roelfes, G. DNA-based hybrid catalysis. *Curr. Opin. Chem. Biol.* **2015**, *25*, 80–87. [CrossRef]
58. Raynal, M.; Ballester, P.; Vidal-Ferran, A.; van Leeuwen, P.W.N.M. Supramolecular catalysis. Part 1: Non-covalent interactions as a tool for building and modifying homogeneous catalysts. *Chem. Soc. Rev.* **2014**, *43*, 1660–1733. [CrossRef] [PubMed]
59. Nakashima, D.; Yamamoto, H. Reversal of Chemoselectivity in Diels-Alder Reaction with α, β-Unsaturated Aldehydes and Ketones Catalyzed by Brønsted Acid or Lewis Acid. *Org. Lett.* **2005**, *7*, 1251–1253. [CrossRef]

60. Chai, J.-D.; Head-Gordon, M. Long-range corrected hybrid density functionals with damped atom-atom dispersion corrections. *Phys. Chem. Chem. Phys.* **2008**, *10*, 6615–6620. [CrossRef] [PubMed]
61. Wiberg, K.B. Ab Initio Molecular Orbital Theory. *J. Comput. Chem.* **1986**, *7*, 379. [CrossRef]
62. Frisch, M.J.; Trucks, G.W.; Schlegel, H.B.; Scuseria, G.E.; Robb, M.A.; Cheeseman, J.R.; Scalmani, G.; Barone, V.; Mennucci, B.; Petersson, G.A.; et al. *Gaussian 09, Revision A.1*; Gaussian, Inc.: Wallingford, CT, USA, 2009. Available online: https://gaussian.com/g09citation/ (accessed on 1 November 2016).
63. Li, Y.; Fang, D.-C. DFT calculations on kinetic data for some [4+2] reactions in solution. *Phys. Chem. Chem. Phys.* **2014**, *16*, 15224. [CrossRef] [PubMed]
64. Fang, D.; Chen, Y. Theoretical Studies on the Mechanism of Cycloaddition Reaction between 1,2,4,5-Tetrazine and Cycloolefines. *Acta Chim. Sin.* **2014**, *72*, 253–256. [CrossRef]
65. Schlegel, H.B. Optimization of equilibrium geometries and transition structures. *J. Comput. Chem.* **1982**, *3*, 214–218. [CrossRef]
66. Schlegel, H.B. Some thoughts on reaction-path following. *J. Chem. Soc. Faraday Trans.* **1994**, *90*, 1569. [CrossRef]
67. Tomasi, J.; Persico, M. Molecular Interactions in Solution: An Overview of Methods Based on Continuous Distributions of the Solvent. *Chem. Rev.* **1994**, *94*, 2027–2094. [CrossRef]
68. Cossi, M.; Barone, V.; Cammi, R.; Tomasi, J. Ab initio study of solvated molecules: A new implementation of the polarizable continuum model. *Chem. Phys. Lett.* **1996**, *255*, 327–335. [CrossRef]
69. Cancès, E.; Mennucci, B.; Tomasi, J. A new integral equation formalism for the polarizable continuum model: Theoretical background and applications to isotropic and anisotropic dielectrics. *J. Chem. Phys.* **1997**, *107*, 3032–3041. [CrossRef]
70. Barone, V.; Cossi, M.; Tomasi, J. Geometry optimization of molecular structures in solution by the polarizable continuum model. *J. Comput. Chem.* **1998**, *19*, 404–417. [CrossRef]
71. Domingo, L.R. A new C-C bond formation model based on the quantum chemical topology of electron density. *RSC Adv.* **2014**, *4*, 32415–32428. [CrossRef]
72. Reed, A.E.; Weinstock, R.B.; Weinhold, F. Natural population analysis. *J. Chem. Phys.* **1985**, *83*, 735–746. [CrossRef]
73. Reed, A.E.; Curtiss, L.A.; Weinhold, F. Intermolecular interactions from a natural bond orbital, donor-acceptor viewpoint. *Chem. Rev.* **1988**, *88*, 899–926. [CrossRef]
74. Domingo, L.; Ríos-Gutiérrez, M.; Pérez, P. Applications of the Conceptual Density Functional Theory Indices to Organic Chemistry Reactivity. *Molecules* **2016**, *21*, 748. [CrossRef]
75. Parr, R.G. Density-Functional Theory of the Electronic Structure of Molecules. *Annu. Rev. Phys. Chem.* **1995**, *46*, 701–728. [CrossRef]
76. Chermette, H. Chemical reactivity indexes in density functional theory. *J. Comput. Chem.* **1999**, *20*, 129–154. [CrossRef]
77. de Proft, F.; Geerlings, P. Conceptual and Computational DFT in the Study of Aromaticity. *Chem. Rev.* **2001**, *101*, 1451–1464. [CrossRef]
78. Geerlings, P.; Proft, F.D.; Langenaeker, W. Conceptual Density Functional Theory. *Chem. Rev.* **2003**, *103*, 1793–1873. [CrossRef]
79. Ayers, P.W.; Anderson, J.S.M.; Bartolotti, L.J. Perturbative perspectives on the chemical reaction prediction problem. *Int. J. Quantum Chem.* **2005**, *101*, 520–534. [CrossRef]
80. Gázquez, J.L. Perspectives on the Density Functional Theory of Chemical Reactivity. *J. Mex. Chem. Soc.* **2008**, *52*, 3–10.
81. Geerlings, P.; Fias, S.; Boisdenghien, Z.; de Proft, F. Conceptual DFT: Chemistry from the linear response function. *Chem. Soc. Rev.* **2014**, *43*, 4989–5008. [CrossRef]
82. Calais, J.-L. Density-functional theory of atoms and molecules. *Int. J. Quantum Chem.* **1993**, *47*, 101. [CrossRef]
83. Domingo, L.R.; Ríos-Gutiérrez, M.; Pérez, P. A molecular electron density theory study of the participation of tetrazines in aza-Diels-Alder reactions. *RSC Adv.* **2020**, *10*, 15394–15405. [CrossRef]
84. Jaramillo, P.; Domingo, L.R.; Chamorro, E.; Pérez, P. A further exploration of a nucleophilicity index based on the gas-phase ionization potentials. *J. Mol. Struct. THEOCHEM* **2008**, *865*, 68–72. [CrossRef]
85. Domingo, L.R.; Pérez, P. The nucleophilicity N index in organic chemistry. *Org. Biomol. Chem.* **2011**, *9*, 7168–7176. [CrossRef] [PubMed]
86. Dennington, R.; Keith, T.; Millam, J. *GaussView, Version 5.0.8*; Semichem Inc.: Shawnee Mission, KS, USA, 2009.